Experimental analysis of airtightness and estimation of building air infiltration using two different single zone air infiltration models

Tijo Joseph, Animesh Dutta

School of Engineering, University of Guelph, Guelph, Ontario, Canada.

Abstract
Building air leakage can contribute significantly to the energy consumption of a building. This paper presents the airtightness performance of a campus building located in Ontario, Canada. The air leakage rate through the building envelope was measured under stilted depressurization conditions following the ASTM E-779 standardized test method. With this test derived empirical leakage flow co-efficient and leakage flow exponent measures, the air infiltration rate for the building under varying wind and outside temperature conditions was calculated using two different single zone air infiltration models – the Lawrence Berkeley Laboratory model and the Alberta Air Infiltration model thus also allowing for a comparison of the results between the two mathematical models.

Keywords: Airtightness; Building air infiltration; Air leakage testing; Single zone infiltration modelling; LBL model; AIM-2 model.

1. Introduction
A building is associated with energy inputs throughout its lifetime but most significantly, during its use phase [1]. In Canada, buildings are estimated to be responsible for around 50% of the total energy used [2]. Importantly though, a substantial amount of energy consumption during a building's operational phase is lost as a waste stream owing to inherent equipment inefficiencies, inadequacies in the design and implementation of the building construction and energy systems, improper maintenance, and not least irresponsible human behavior. On the other hand, these factors can lead to a higher than best case scenario building energy demand. Building air leakage is an important pathway that can result in energy loss or contribute to a higher energy consumption. It is only pertinent therefore to qualify and quantify the air leakage in buildings.
Primarily, there are three means by which an air exchange can occur between the interior and exterior of a building envelope; by natural ventilation, by infiltration (or exfiltration) or by mechanical ventilation. Natural ventilation, typically intentional, allows for outdoor air ingress into the building through fenestration. Mechanical ventilation can facilitate the exchange of air across the envelope with the operation of an exhaust or supply fan. Unlike these two means, infiltration or exfiltration is unplanned for and represents the leakage of air through openings in the building fabric. While infiltration represents flow from the exterior of the building to the interior, exfiltration stands for the reverse. In this paper, infiltration may be used to mean both infiltration and exfiltration.

Various studies have reported the impact of air leakage on building energy demand. In a parametric computer simulation study of residential building prototypes in the United States (USA), the authors estimated infiltration as one of the two major components of heat loss from buildings [3]. In terms of heat gain, the same study estimated the contribution from infiltration as around 16% [3]. In a study based in Finland, infiltration was reported to contribute to 15 to 30% of the energy consumed for space heating purposes [4]. A thirteen country European study attributed around 53% of space heating as going into leakage loss [5]. In a study of commercial buildings in the USA, the contribution of infiltration to energy demand was reported as ranging from 10% to 42% with the higher impact observed in cold climates[6]. In yet another study on commercial building prototypes, the results indicated that infiltration was one of the biggest contributors to heating loads [7].

Evidently, infiltration or exfiltration can impact and is a major source of the heating and to a lesser extent the cooling load requirements of a building [6, 8-10]. In the case of cooling loads though, infiltration under the right circumstances can offset some of the load requirement [9]. Whether free cooling provided by infiltration can be availed of is a matter of local climatic conditions [9]. For example, in regions where the humidity is very high, moisture laden air infiltration can result in the build-up of moisture levels within the building [9]. Ultimately, this may warrant interior dehumidification.

Air infiltration under conducive conditions can also indirectly result in damage to components of the building envelope. Air laden with moisture can seep into wall assemblies or into the interior of the building thereby contributing to potential moisture related issues like mold or rot formation [11, 12]. The contribution of infiltration to the ventilation requirements of building occupants and also to indoor air quality(IAQ) is yet another factor that underscores the relevance of airtightness studies for buildings [8, 10, 12]. In general though, it is desirable to reduce air infiltration in buildings as it can significantly contribute to the energy consumption of a building [13]. This narrates the importance of studying the air leakage characteristics of buildings. This paper presents the results from an experimental analysis of the airtightness of a campus building and further, also estimates the air infiltration rate for the building under varying climatic conditions.

2. Building details

The campus building under investigation is a historic two storied building with a look-out basement and was built circa 1882. The building is located in the Canadian province of Ontario (Figure 1). It has a gross floor area of 3478 square feet (sq.ft.) and a net floor area of 3090 sq.ft and can be classed as similar to a residential type building. The building height is around 7 meters (m) and the base shape is rectangular with a length to breadth sizing of 10.3m by 14.8m. The total conditioned volume for the building is around 596 cubic meters (m^3). The building is oriented in the north-east direction with a site altitude of 338m, and latitude and longitude references as 43° 31'53.03" and 80^o13'34.17" respectively. The building is not serviced by any air conditioning or ventilation equipment and thus air ducts are not present.

Figure 1. Campus building located in Ontario, Canada

3. Pathways, drivers &characteristics of air leakage in buildings

There are various elements that shape the airtightness of a building and this includes the building foundation type, ventilation scheme, number of floors, how complex the building envelope is and not least the construction quality [14, 15]. The air leakage pathways for a building can be in the form of cracks in the building envelope, holes in the components of the building fabric or gaps in the interface between building elements. Typically, air leakage can occur through the walls, at the intersection between the wall and the floor or ceiling, at interfaces to the attic, basement or crawlspace and also at spots where non-effectively sealed off penetrations run through the air barrier [14, 16]. Air leakage can also occur around and through fenestration, around electrical switches and power outlets, through the fireplace chimney, and also through the heating, ventilation and air-conditioning (HVAC) ducts [14]. Table 1 provides an estimate of the dispersion of air leakage across different elements of a building as cited in the ASHRAE handbook of fundamentals [17].

Table 1. Air leakage distribution across building elements [17]

Component description	% Distribution range
Walls	18% – 50%
Ceiling	3% to 30%
HVAC	3% – 28%
Fenestration	6% - 22%
Fireplace	0% - 30%
Exhaust vents in conditioned spaces	2% - 12%

Building air leakage is fundamentally driven by a pressure or temperature differential or, a combination of both, between the building indoor and outdoor environments. In any case, this leads to a resultant pressure differential across the building envelope and is a result of one or a combination of the following occurrences: wind blowing onto a building facade, the stack effect phenomenon or the operation of in-house mechanical devices such as an exhaust fan [11]. Exhaust fans for example, in the process of pulling out and exhausting interior air, can result in depressurizing the building interior and consequently pulling in outside air into the building. Stack effect is the result of a temperature differential between the exterior and interior of the building and is more pronounced with building height and a higher temperature difference [11]. Stack effect is also the major contributor of infiltration in buildings [18].

Generally, the flow characteristics of air infiltration, that is, whether laminar or turbulent, the dispersion and physical magnitude of the leakage paths and the pressure differential between the interior and exterior of the building influences the air leakage rate through the building envelope [19]. The infiltration rate depends on the weather conditions and is a variable subject to daily and seasonal variations throughout the year [15, 20].Under stack effect, buoyant warm air in the interior of the building rises and can escape from leakage areas located at the top level of the building [11]. This simultaneously draws in cold air through leakage points at the base level. This is the case during winter. However in summer, the stack effect operates in reverse but is much less pronounced than is the case in winter. In the reverse scenario, cold air drops to the lower level of the building and thereby draws out this generally conditioned indoor air through the leakage areas at the base level [11]. Typically with stack effect, a neutral pressure plane develops where the switch occurs from exfiltration to infiltration over the building height.

Wind induced infiltration develops as wind blows over a building thus working up pressure on the windward side. Wind is thus pushed in through leakage areas on the respective windward facade and at the same time results in air flowing out from the leeward end [12]. Wind is variable in nature both in terms of velocity and direction and thus so is the infiltration behavior induced by wind. In general, based on average wind speeds of 10 to 15mph, the average annual wind induced pressure differential is reported as ranging from 10 to 14Pascal(Pa) [12]. The local terrain features and the building shape also influences wind induced air leakage [11].

4. Airtightness measurement methodology

A mass balance approach to airflow across the building envelope along with details of the leak path characteristics derived using approximate methods, forms the basis of estimating the total air leakage of a

building [15, 19]. There are different standards that define the measurement methodology for ascertaining the airtightness of a building. This includes the CGSB 149.10-M86 'Determination of the Airtightness of Building Envelopes by the Fan Depressurization Method' standard, the ASTM E-779 'Standard test method for Determining Air Leakage Rate by Fan Pressurization' standard or the ISO 9972 'Thermal Insulation - Determination of Building Airtightness - Fan Pressurization Method' standard.

The ASTM standard E-779,selected as the reference standard for this investigation, defines a standardized test methodology for measuring the air leakage rate through a building envelope under controlled depressurization conditions [8]. A fan induced depressurization is carried out typically using a blower door assembly to move air through the building envelope. The blower door unit has a variable speed controlled calibrated fan. When the fan is run under depressurization mode thus blowing air out of the building, the resultant is an artificial pressure differential between the building interior and exterior [18].

Depressurization is applied under single zoning to the building envelope at different relatively high pressures ranging between 10 to 60Pa and the corresponding steady-state airflow through the building envelope, required to maintain a stable pressure differential, is logged [16]. An airflow and pressure differential measuring system provides the required measurement data. The high test pressures serve to mitigate the effect of wind or stack effect [18]. The relationship between the depressurization values and the corresponding logged airflow rates forms the basis of deriving a leakage flow exponent (n) and leakage flow coefficient (C) which can then be used to estimate the airtightness or effective leakage area(ELA) of the building [8, 20].

The ASTM standard E-779 also defines certain limiting conditions above which depressurization testing will not yield good results. The first condition is to ascertain if the stack effect is too pronounced and is based on checking if the product of interior-exterior temperature differential in absolute terms and the building height is greater than $200m^{o}C$. The second recommendation is pertaining to desirable outside environmental conditions; which is wind speeds of 0 to 2m/s and temperatures ranging between 5 to $35^{o}C$.

In this study, a Minneapolis Blower Door^{TM}(Model 3) system along with a DG-700 pressure and flow gauge was used to conduct the airtightness test. The blower unit and the pressure and flow gauge are depicted in Figure 2. After set-up procedures were completed including zeroing for building baseline pressure correction, the building was subjected, as a single zone, to a multi-point depressurization test with the test procedures following the ASTM E779 standard. Air leakage data, as cubic feet per minute (CFM), was logged for varying pressures subject to a ten seconds time averaging function available with the DG 700 unit. Interior and exterior temperatures were logged during the testing. Local wind speed was also noted using a vane anemometer to ensure test conditions conformed to the ASTM E779 standard. The reference standard conditions of temperature as $20^{o}C$ and air density as $1.2041kg/m^3$ applied.

Figure 2. Minneapolis model 3 blower unit and a DG-700 digital gauge

An empirical relationship which takes the form of a power law function, $Q = C\Delta P^n$, generally describes the infiltration flow across the building envelope [15, 20, 21, 22]. Data obtained from the blower door testing can be reduced to this empirical relationship between airflow (Q) and the corresponding pressure differential (ΔP). It is relevant to note that the blower door data indicates the leakage rate under stilted status and does not represent infiltration rate as yet [15, 20]. The power law function can be used to forecast the infiltration under normal conditions [15, 20, 21]. The flow exponent n and the flow coefficient C are empirical measures representing the building leakage characteristics and are specific to the building. These empirical values stand for the leakage sizing, leakage path and airflow regime present in the building [15, 20].

5. Estimating air infiltration under varying climatic conditions

Based on the empirical C & n measures and or the estimated leakage area provided by the depressurization test, there are different approaches in estimating the building air infiltration rate under typical local environmental conditions [10]. For buildings modeled as a single zone, one of these approaches is to use a single zone superposition model [19]. In this paper, two such air infiltration models, namely the Alberta air infiltration (AIM-2) model and the Lawrence Berkeley Laboratory (LBL) model, are used to estimate the air infiltration rate for the studied building under varying wind and outside temperature conditions. This also allows for a comparative assessment of the results from the two mathematical infiltration models.

The AIM-2 model singly works out the airflow associated with wind and likewise due to stack effect and then calculates the combined effect using a superposition equation [23]. The model is based on the $Q = C\Delta P^n$ empirical relationship and in addition, accounts for the flue outlet of the building as a separate leakage area. However, for this study, the flue outlet parameters required in the model are not considered as the building under investigation does not have any flue outlets. The C & n values are required inputs to the model. Another model input is based on defining the leakage distribution in the building envelope in terms of fractions of the total leakage. A uniform leakage distribution is assumed in this case. The wind speed, another required input, is considered at eaves height of the building [23]. The wind shelter factor which represents the local shielding effect around the building is assigned the shelter type 'light local shielding' based on the observed site topography [23].

The LBL model describes the infiltration in a building taking into account the leakage characteristics established through blower door diagnostics and then accounts for infiltration driving forces due to wind and temperature climatic conditions [15, 20]. One of the required parameters for the LBL model is ELA. ELA stands for the area of a nozzle shaped hole which has a discharge coefficient of 1 and which, on an equivalent basis, can result in the same infiltration rate as is the case for the building under a 4Pa pressure differential [15, 20, 21]. As with the previous model, a uniform leakage distribution is assumed. A generalized shielding coefficient parameter based on the local shielding present is also a model input and for this case, a 'light local shielding with few obstructions' category value is assigned [15, 20]. A 'terrain class III' is selected as terrain classification towards assigning the terrain class parameters in the model [15, 20].

Two climatic aspects for the site, which are required inputs for both the superposition air infiltration models, were also examined. One is the average daily temperature range observed locally and the other is the local wind speed trend. Historical averages climate data (1971 to 2000) from the Guelph Arboretum weather station gives the average daily temperature as ranging from lows of $-11^{\circ}C$ to highs of $26^{\circ}C$ [24]. For the wind trend, the wind rose diagram for the site was generated based on typical metrological year (TMY) and modelled weather data using Autodesk® Vasari's wind rose tool. The overlaid wind rose diagrams on the building site for two separate periods - November to the following March (winter) and May to September (summer)is given in Figure 3 and provides information on the frequency and speed of wind at the site. From the wind rose diagram, it is evident the site experiences wind speeds as high as +7m/s and chiefly from a west direction.
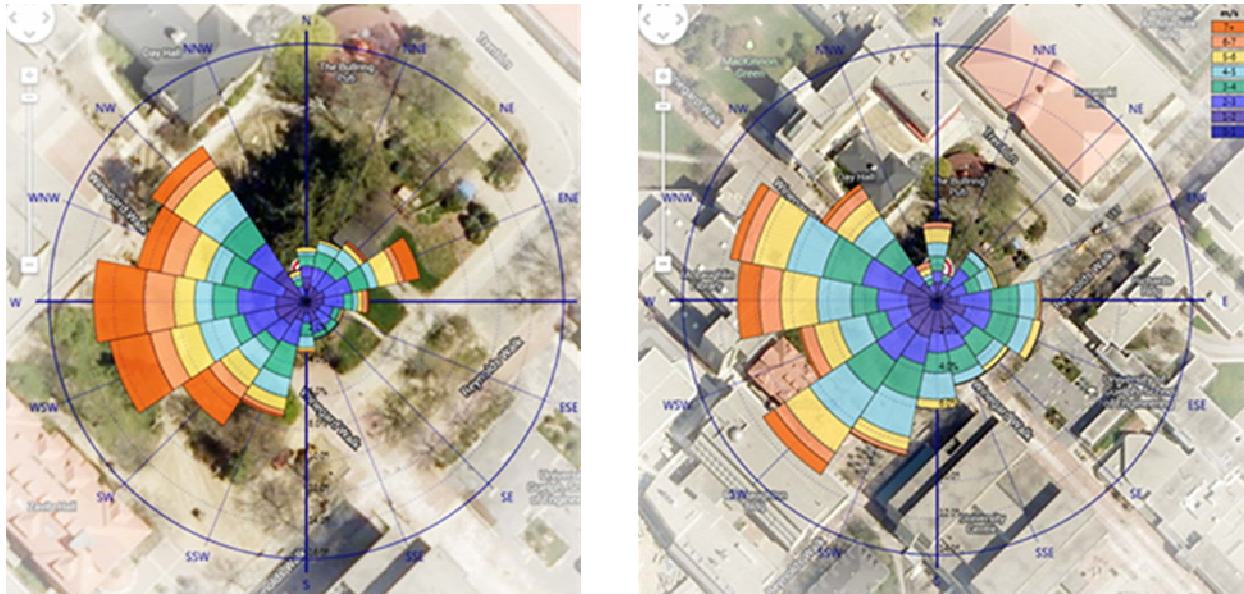
Figure 3. Wind rose diagrams for the building site over winter and summer periods [Courtesy – *Autodesk® Vasari*]

6. Airtightness field measurement data and air change per hour standards

In order to ensure a standard basis for comparison, or put another way, for the fact that buildings having a larger wall, floor or roof area have more potential for leakage spots, air leakage results are typically normalized in terms of volume or area [25]. Air change per hour (ACH) is one such measure and represents the frequency of air replacement within the building on a per hour basis [18]. The corresponding ACH under 50Pa is termed ACH50. Table 2 is a summary of the observed range of air change rate values at 50Pa from field measurements carried out in Canada covering residential buildings.

Table 2. ACH50 field measurement data for Canada

Sample Size	Range for ACH50 (/hr)		Reference
	Lower	Upper	
222	0.4	11	[26]
47	0.13	2.6	[26]
100	1.876	4.653	[25]

A review of airtightness field measurements carried out in Europe and North America for residential buildings reports a wide range from 0.5 to 84 hr^{-1} @ ACH50 [14, 25, 27-31]. In a survey study of airtightness measurements carried out on buildings in Canada, the authors reported a typical average value of 4.4hr^{-1} @ ACH50 for residential buildings and a range of 1.1 to 1.6hr^{-1} @ ACH50 for commercial buildings [32]. As far as standards, there are various airtightness standards across different countries. These standards also differ in the quoted maximum permissible air change rate. The R-2000 standard in Canada is set at 1.5hr^{-1} @ ACH50 [33]. Examining standards in Europe gives a range of 0.5 to 6hr^{-1} @ ACH50 as the standard limit for allowable air change rate [27].

7. Results and discussion

The measurement data from the blower door test, corrected for baseline pressure, site altitude and air density using a proprietary software (TECTITE^{TM}) provided by the blower door manufacturer, is presented in Figure 4.

Based on this data, and using the calculation methodology provided in the ASTM E779 standard, the following measures are obtained:

Flow coefficient, C = 0.246 m^3/(sPa^n)

Flow exponent, n = 0.6

95% confidence limit for n = 0.012 & 95% confidence limit for ln(C) = 0.044

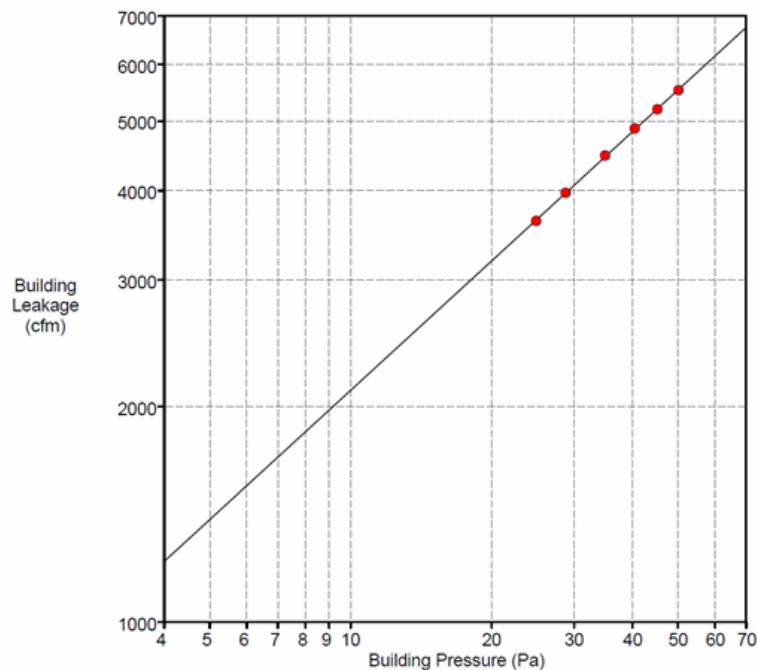Effective leakage area, ELA = 0.215m^2

Figure 4. Depressurization testing– CFM versus building pressure (Courtesy – *TECTITE[TM] software*)

Guided by information provided in Chan et al., 2013 [34],the obtained n value of 0.6 indicates that the leakage sites in the building are constituted predominantly of "specific openings". The ELA value of $0.215m^2$ represents the cumulative sizing of the leakage areas in the building. To set this in better perspective, the area of a window in the main section of the building is around $1.46m^2$. The TECTITE[TM] software generated ACH50 value for the building based on the blower door test data is $15.5hr^{-1}$. Taking into consideration the limit set by the R-2000 standard for permissible air change rate ($1.5hr^{-1}$@ ACH50), this obtained building ACH50 value does not meet the standard and also establishes that the building is leaky. Based on a building leakage characterization table (covering leakage class A to J corresponding to ACH50 values of $1hr^{-1}$ and $>27hr^{-1}$ respectively) provided in Sherman, 1995 [20], the campus building can be categorized as of leakage class G. According to EN ISO 13790, if the ACH50 is greater than 10 under natural infiltration conditions, which is the case here, the building would be categorized as having a low envelope tightness level [35].

Based on the site wind speed range as depicted in the wind rose plots and the potential daily average maximum temperature differential between the exterior temperature and expected interior set point temperature of the building, the AIM-2 infiltration model is used to obtain the cumulative effect airflow rate (Q, derived from superposition of the stack related Q_s and wind related Q_w airflow rates) and the corresponding ACH values. The variation of these obtained values versus wind speed and temperature differential are presented as plots in Figures 5 to 8. As observed from Figure 6, with the temperature differential assumed to be holding at a constant of 17^oK, the estimated ACH value increases from around 1ACH to 2.75ACH corresponding to a wind speed change from 1m/s to 8m/s. On the other hand, with the wind speed assumed to be holding at a constant of 2m/s, the estimated ACH value drops from a high of 1.6ACH to a low of around 0.6ACH corresponding to temperature differentials of 37^oK and 2^oK respectively. Additionally, the ACH values are also estimated using the LBL model. There is a difference in the airflow rate and ACH estimations made by the two mathematical models and this is summarized in Tables 3 and 4. The ACH estimation difference between the two models range as high as 31%.
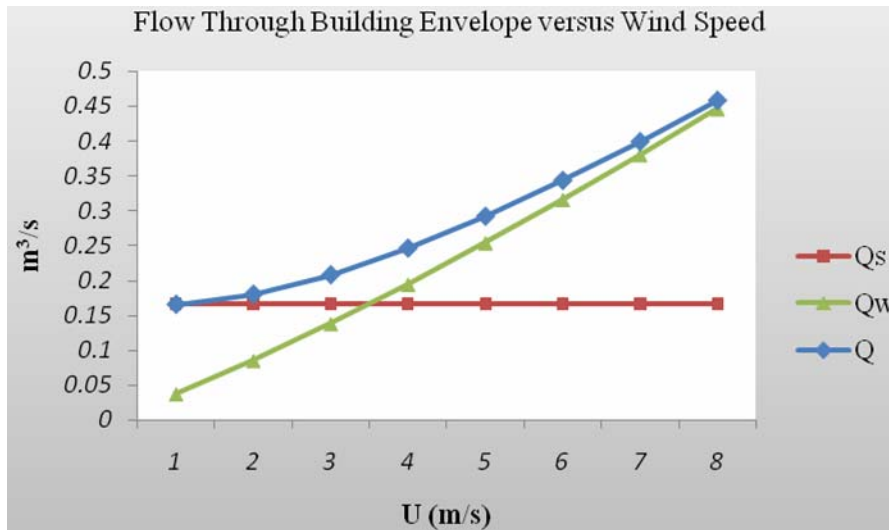
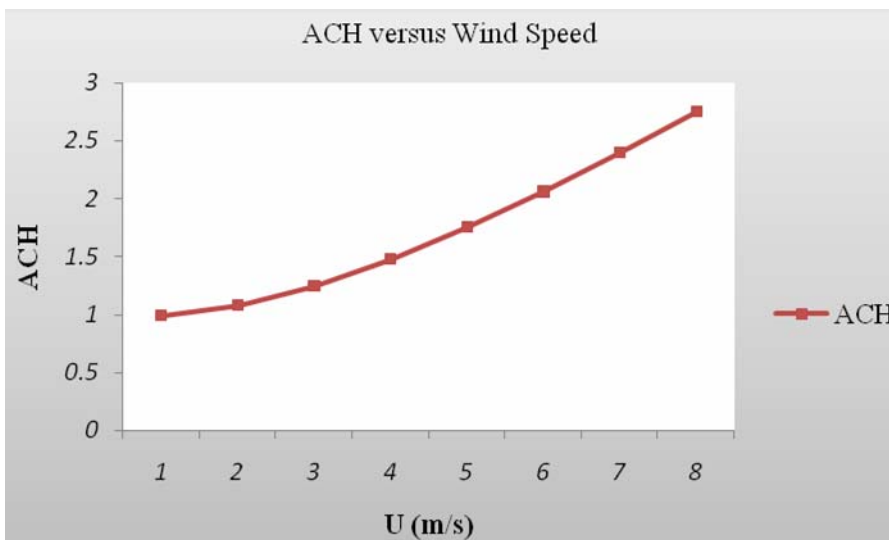Figure 5. Stackrelated (Q_s), wind related (Q_w)&cumulative effect (Q) airflow rate versus wind speed

Figure 6. ACH versus wind speed
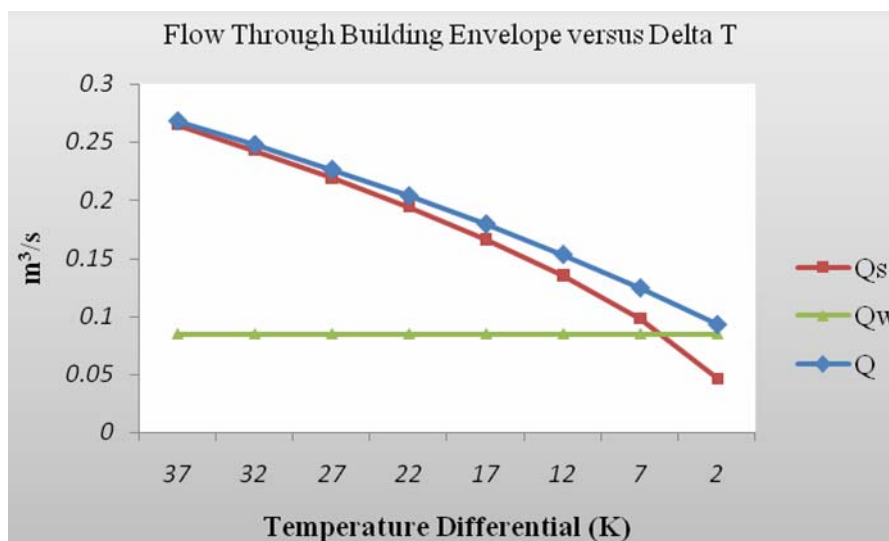

Figure 7. Stack related (Q_s), wind related (Q_w) & cumulative effect (Q) airflow rate versus temperature differential
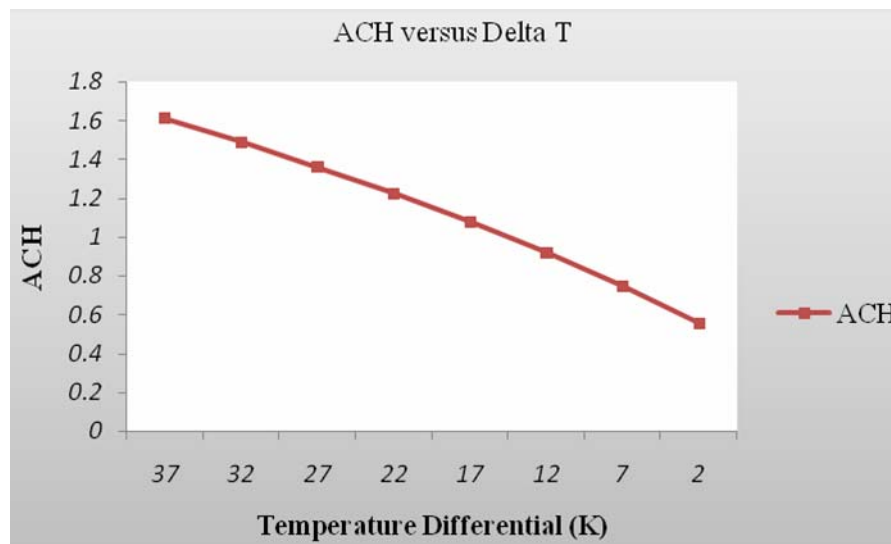
Figure 8. ACH versus temperature differential

Table 3. Difference in estimation of airflow rates between LBL and AIM-2 models

v' (m/s)	Q_w (m³/s) (*LBL*)	Q_w (m³/s) (*AIM*)	Difference - AIM over LBL %	ΔT (K)	Q_s (m³/s) (*LBL*)	Q_s (m³/s) (*AIM*)	Difference - AIM over LBL %
1	0.038	0.037	2%	37	0.262	0.265	-1%
2	0.075	0.085	-12%	32	0.243	0.243	0%
3	0.113	0.137	-22%	27	0.224	0.220	2%
4	0.151	0.194	-29%	22	0.202	0.194	4%
5	0.188	0.254	-35%	17	0.177	0.166	6%
6	0.226	0.316	-40%	12	0.149	0.135	9%
7	0.264	0.380	-44%	7	0.114	0.098	14%
8	0.301	0.446	-48%	2	0.061	0.046	24%

Table 4. Difference in estimation of ACH between LBL and AIM-2 models

v' (m/s)	ACH (hr⁻¹) (*LBL*)	ACH (hr⁻¹) (*AIM*)	Difference - AIM over LBL %	ΔT (K)	ACH (hr⁻¹) (*LBL*)	ACH (hr⁻¹) (*AIM*)	Difference - AIM over LBL %
1	1.09	0.99	9%	37	1.63	1.61	1%
2	1.16	1.08	7%	32	1.53	1.49	3%
3	1.26	1.24	1%	27	1.41	1.36	4%
4	1.40	1.47	-6%	22	1.29	1.22	5%
5	1.55	1.75	-13%	17	1.16	1.08	7%
6	1.72	2.06	-20%	12	1.00	0.92	8%
7	1.91	2.40	-26%	7	0.82	0.74	9%
8	2.10	2.75	-31%	2	0.58	0.55	4%

8. Conclusions

Having investigated the airtightness performance of the campus building, the following describe the key conclusions and follow-up recommendation:

- The reported building ACH50 value of 15.5hr⁻¹, when compared to the ACH50 range observed from field measurements for residential buildings across Canada (0.13hr⁻¹ to 11hr⁻¹), is a clear outlier. The

building ACH50 value also far exceeds the R-2000 standard permissible air change rate of 1.5hr^{-1} at ACH50.

- The estimated ELA for the building is 0.215m^2 and the nature of the leakage sites is assessed as 'specific openings'.
- Even with accounting for potential uncertainties in the test results including with flow or pressure recordings (the DG 700 specification sheet reports a flow accuracy of +/-3%) or with normalizing the test data to the conditioned volume, the campus building can conclusively be categorized as having a low envelope tightness level. This effectively translates to energy loss for the building during the heating season.
- The ACH range exhibited against varying wind speed and interior – exterior temperature differentials typical at the building site, is estimated using two different single zone air infiltration models, the AIM-2 model and the LBL model, to also allow for model intercomparison. The resultant plots indicate an ACH ranging from 1hr^{-1} to 2.75hr^{-1} against wind speeds in the range of 1 to 8m/s and a range of 0.5hr^{-1} to 1.6hr^{-1} corresponding to a temperature differential range of 2°K to 37°K. There is an ACH estimation difference between the two models and this ranges as high as 31% in the case of varying wind speed conditions, but is relatively narrower registering a high of 10% in the case of varying temperature differentials.
- The air infiltration modeling result is based on assumptions made with regards to the leakage distribution in the building. Identification of the leakage pathways in the building can allow for a revised assignment of the leakage distribution so as to reflect the actual case.
- In light of this airtightness study which classes the investigated building as leaky, it is recommended, as an energy conservation measure, to further investigate the building envelope using methods like smoke tracing and or infrared thermography towards identifying the air leakage pathways and applying retro-fit measures in addressing these leakage sites.

References

[1] Perez-Lombard, L., Ortiz, J., & Pout, C. (2008). A review on buildings energy consumption information. Energy and Buildings, 40(3), 394-398.

[2] Natural Resources Canada's Office of Energy Efficiency. (2011).Comprehensive Energy Use Database, 1990 to 2011. Retrieved April18, 2014, from
http://oee.nrcan.gc.ca/corporate/statistics/neud/dpa/comprehensive_tables/list.cfm?attr=0

[3] Huang, J., Hanford, J., & Yang, F. (1999). LBNL-44636 Residential heating and cooling loads component analysis. California: Building Technologies Department, Environmental Energy Technologies Division, Lawrence Berkeley National Laboratory, University of California.

[4] Jokisalo, J., Kurnitski, J., Korpi, M., Kalamees, T., & Vinha, J. (2009). Building leakage, infiltration, and energy performance analyses for Finnish detached houses. Building and Environment, 44(2), 377-387.

[5] Orme, M. (2001). Estimates of the energy impact of ventilation and associated financial expenditures. Energy and Buildings, 33(3), 199-205.

[6] Emmerich, S. J., McDowell, T. P., & Anis, W. (2005). Investigation of the impact of commercial building envelope airtightness on HVAC energy use. US Department of Commerce, Technology Administration, National Institute of Standards and Technology.

[7] Huang, Y. J., & Zhang, H. (1999). Commercial heating and cooling loads component analysis. Energy Analysis Program, 7.

[8] ASTM Standard E779, 2003, "Standard Test Method for Determining Air Leakage Rate by Fan Pressurization," ASTM International, West Conshohocken, PA, 2003, DOI: 10.1520/E0779-03, www.astm.org.

[9] Rasouli, M., Ge, G., Simonson, C. J., & Besant, R. W. (2012). Uncertainties in energy and economic performance of HVAC systems and energy recovery ventilators due to uncertainties in building and HVAC parameters. Applied Thermal Engineering, 50(1), 732-742.

[10] Wang, W., Beausoleil-Morrison, I., & Reardon, J. (2009). Evaluation of the Alberta air infiltration model using measurements and inter-model comparisons. Building and Environment, 44(2), 309-318.

[11] Building Energy Codes. (2011). Building Energy Code Resource Guide: Air Leakage Guide. Catalogue No. PNNL-SA-82900. U.S.A.: U.S. Department of Energy.

[12] Anis, W., & Wiss, F. A. I. A. (2006). Air barrier systems in buildings. Whole Building Design Guide, National Institute of Building Science.

[13] Alfano, F. R., Dell'Isola, M., Ficco, G., & Tassini, F. (2012). Experimental analysis of air tightness in Mediterranean buildings using the fan pressurization method. Building and Environment, 53, 16-25.

[14] Kalamees, T. (2007). Air tightness and air leakages of new lightweight single-family detached houses in Estonia. Building and Environment, 42(6), 2369-2377.

[15] Sherman, M. H. (1987). Estimation of infiltration from leakage and climate indicators. Energy and Buildings, 10(1), 81-86.

[16] Sherman, M. H., & Chan, W. R. (2004). Building airtightness: research and practice. LBNL report, 53356.

[17] ASHRAE. Infiltration and ventilation requirements, Ch. 27 of ASHRAE handbook of fundamentals. Atlanta: American Society of Heating, Refrigerating and Air Conditioning Engineers; 2009.

[18] Minneapolis Blower Door® Operation Manual for Model 3 and Model 4 Systems. Energy Conservatory.

[19] Awbi, H. B. (2003). Ventilation of buildings (2nd ed.). New York: Spon Press.

[20] Sherman, M. (1995). The Use of Blower-Door Data. Indoor Air, 5(3), 215-224.

[21] Persily, A. K. (1998). Airtightness of commercial and institutional buildings: blowing holes in the myth of tight buildings. Building and Fire Research Laboratory, National Institute of Standards and Technology.

[22] The Energy Conservatory. (2014). Automated Blower Door Systems and Accessories. Retrieved April 18, 2014, from http://www.energyconservatory.com/products/automated-blower-door-systems-and-accessories

[23] Walker, I. S., & Wilson, D. J. (1998). Field validation of algebraic equations for stack and wind driven air infiltration calculations. HVAC&R Research, 4(2), 119-139.

[24] Government of Canada. Calculation of the 1981 to 2010 Climate Normals for Canada. Retrieved April 18, 2014, from http://climate.weather.gc.ca/climate_normals/normals_documentation_e.html

[25] Harris, J. (2009). Air Leakage in Ontario Housing. Retrieved April 18, 2014, from http://www.mah.gov.on.ca/Asset8296.aspx?method=1

[26] Hamlin T. (1997). Airtightness and Energy Efficiency of New Conventional & R-2000 Housing in Canada. Ottawa, ON: Canada Centre for Mineral and Energy Technology, Natural Resources Canada.

[27] Pan, W. (2010). Relationships between air-tightness and its influencing factors of post-2006 new-build dwellings in the UK. Building and Environment, 45(11), 2387-2399.

[28] Persily, A., Musser, A., Emmerich, S.J. (2010). Modeled infiltration rate distributions for US housing. Indoor Air, 20(6), 473-485.

[29] Blomsterberg, Å., Carlsson, T., Svensson, C., & Kronvall, J. (1999). Air flows in dwellings-simulations and measurements. Energy and buildings, 30(1), 87-95.

[30] Jokisalo, J., Kalamees, T., Kurnitski, J., Eskola, L., Jokiranta, K., & Vinha, J. (2008). A comparison of measured and simulated air pressure conditions of a detached house in a cold climate. Journal of Building Physics, 32(1), 67-89.

[31] Juodis, E. (2000). Energy saving and airtightness of blocks of flats in Lithuania. Indoor and Built Environment, 9(3-4), 143-147.

[32] Fennell, H. C., & Haehnel, J. (2005). Setting airtightness standards. ASHRAE journal, 47(9), 26.

[33] Natural Resources Canada. (2012). More information on the R-2000 Standard. Retrieved April 18, 2014, from https://www.nrcan.gc.ca/energy/efficiency/housing/new-homes/5089

[34] Chan, W. R., Joh, J., & Sherman, M. H. (2013). Analysis of air leakage measurements of US houses. Energy and Buildings, 66, 616-625.

[35] Sfakianaki, A., Pavlou, K., Santamouris, M., Livada, I., Assimakopoulos, M. N., Mantas, P., & Christakopoulos, A. (2008). Air tightness measurements of residential houses in Athens, Greece. Building and Environment, 43(4), 398-405.

Tijo Joseph received his MSc in Automotive Engineering from University of Hertfordshire, UK (2001), PGDip in Energy Management from MITSDE, India (2011) and MEng in Environmental Engineering from University of Guelph, Canada (2013). He is currently a researcher at the University of Guelph and his research interest covers topics in energy engineering including energy management, energy auditing, energy conservation, life cycle assessment and sustainability in buildings.
E-mail address: tjoseph@uoguelph.ca

Animesh Dutta is an Associate Professor with the School of Engineering at the University of Guelph. He has a PhD in Mechanical Engineering from Dalhousie University (Canada).His research interests include boiler design, fluidized bed technology, biomass and agri-residue processing and conversion, renewable and clean energy technologies, design and assessment of advanced energy systems, life cycle analysis and thermodynamic optimization. To date, he is the author of 112 publications including 40 refereed journals and 31 refereed conference proceedings.
E-mail address: adutta@uoguelph.ca